SEISMIC PERFORMANCE AND RESILIENCE COMPARISON OF THREE DESIGNS OF A HYPOTHETICAL 6-STORY STEEL BUILDING IN LOS ANGELES: SPECIAL MOMENT FRAME (SMF), BASE ISOLATED SMF, AND SMF WITH VISCOUS DAMPERS

Gabriel Acero, MSSE, SE, Senior Associate, AECOM
Chair of SEAOSC Seismology and Hazards Committee, Chair of SIED
Orange, California, USA

Nathan Canney, Ph.D., PE., Director of Structural Engineering, Taylor Devices, Inc.
Sacramento, California, USA

Steven R. Shepherd, S.E., Senior Project Manager, Simpson, Gumpertz & Heger
Member of SEAOSC Seismology and Hazards Committee
Newport Beach, California, USA

Jesse Karns, SE., Principal Structural Engineer - R&D at MiTek, Inc.
Past-Chair of SEAOSC Seismology and Hazards Committee
Mission Viejo, California, USA

Martin B. Hudson, Ph.D., PE, GE., Adjunct Professor, University of California, Los Angeles
Principal Geotechnical Engineer, Hudson Geotechnics, Inc.
SEAOSC Honorary Member and Member of SEAOSC Seismology and Hazards Committee
El Segundo, California, USA

Ady Aviram, Ph.D., P.E., Regional Director –Earthquake Protection Systems EPS, California, USA

Marios Panagiotou, Ph. D., PE., Structural Engineer, Lawrence Livermore National Laboratory
Member of SEAOSC Seismology and Hazards Committee
Livermore, California, USA

Anoop S. Mokha, Ph.D., S.E., Vice-President - Earthquake Protection Systems EPS, California, USA

Cairo Briceno, MSc, SE., Senior Supervising Struct. Engineer, Parsons
Co-Chair of SEAOSC Seismology and Hazards Committee
Los Angeles, California, USA

Victor Garcia-Delgado, Ph. D., SE.,Senior Struct. Engineer, Division of the State Architect (DSA), Ret.,
Past Chair of SEAOSD Seismology Committee
San Diego, California, USA,

Marija Trifunovic, M.Sc., Regional Director –Earthquake Protection Systems EPS, California, USA.

Note:

1. All authors are active members of the Seismology Committee of the Structural Engineers Association of California, SEAOC, and the Seismic Isolation and Energy Dissipation Task Committee, SIED.
2. SEAOSC stands for the Structural Engineers Association of Southern California.

Abstract

This paper studies the seismic performance and resilience of three different designs of a hypothetical six-story steel building located at a near-fault site in Los Angeles, California. The three lateral seismic resistance systems evaluated satisfy the requirements of ASCE 7-22 (ASCE 7, basis of the International Building Code, IBC-24) and are: (i) fixed-base Special Moment Frame (SMF or FB-SMF); (ii) SMF base isolated with triple friction pendulums isolators (BI-SMF); and (iii) SMF with fluid viscous dampers (SMF-VD). All three buildings are designed to satisfy the minimum requirements of ASCE 7 [13] for a Risk Category II building.

The three buildings are analyzed by performing three-dimensional nonlinear response history analysis (NLRHA), using ETABS, for a set of 11 site specific ground motions developed for the design earthquake (DE) as well as risk-targeted maximum considered earthquake (MCE_R). The nonlinear behavior of the isolation and viscous damping devices as well as that of the SMF beam and column hinges are explicitly modeled. The response is quantified in terms of story shear forces, drifts (peak and residual), floor accelerations, displacement and forces of the isolators and the dampers. Approximate construction cost differences between the three building types are discussed. The limitations of code-minimum analysis procedures for the fixed-base SMF are demonstrated from the comparison with NLRHA. A seismic loss and functional recovery time comparison is conducted using the FEMA P-58 and ATC-138 frameworks implemented in the SP3 computational platform to evaluate the resiliency of the designs.

Introduction

Seismic isolation and energy dissipation technologies for buildings represent a well-established and extensively validated field, underpinned by more than four decades of analytical research, experimental investigations, and global applications [1–12]. Through rigorous laboratory testing and advanced computational modeling, devices such as laminated rubber bearings, friction bearings, frictional interfaces, and fluid viscous dampers [14] have been shown to be economically viable solutions capable of withstanding the combined displacement and force demands imposed by seismic events, including near-fault regions.

The efficacy of base isolation systems arises from their ability to localize lateral deformations within strategically engineered isolation interfaces. This mechanism facilitates an essentially elastic dynamic response in the superstructure by concentrating energy dissipation and inter-story displacement within the isolators. Consequently, the intervention significantly mitigates higher-mode excitations, thereby reducing associated inter-story shears and floor accelerations throughout the structure. The application of fluid viscous dampers, on the other hand, supplements hysteretic damping throughout the building with viscous damping, decreasing damage in the lateral-force resisting components, inter-story drift and peak floor acceleration. Distributed damping throughout the full height of the building is most common, where damping devices span between two floors and utilize the relative movement between the floors to drive a piston head through a viscous fluid (like silicone or oil).

Despite the proven efficacy of seismic isolation and energy dissipation systems, their adoption within the United States remains limited, with only a small fraction of structures utilizing such technologies [11]. The vast majority of buildings (including major buildings) continue to be designed in accordance with the code-minimum provisions set forth in ASCE 7 [13], which do not mandate the implementation of seismic isolation. The seismic performance anticipated under ASCE 7 corresponds, for Risk Category II structures (normal occupancy), to a limited conditional probability of collapse of approximately 10% during a risk-targeted Maximum Considered Earthquake (MCE_R), characterized by a return period of 2,475 years and a deterministic upper bound at the 84th percentile. Code-compliant seismic design relies on the application of a response modification factor, R, and equivalent linear analysis to estimate seismic forces associated with the Design Earthquake (DE), defined as possessing spectral accelerations equivalent to two-thirds of those at MCE_R levels. However, the code-minimum design approach does not incorporate explicit metrics of seismic resilience, such as quantification of post-event damage, economic losses, or timelines for functional recovery—elements that are critical to performance-based engineering frameworks and holistic risk mitigation strategies.

In this study we compare the seismic performance and resilience of three seismic designs of a six-story steel frame building located at a near-fault site in California: (i) a fixed-base special moment frame (SMF), (ii) a base-isolated SMF using triple pendulum bearings (BI-SMF); and (iii) a fixed-based SMF with supplemental damping using fluid viscous dampers (SMF-VD). Nonlinear Response History Analysis (NLRHA) was employed to derive high-fidelity estimates of structural response under both Design Earthquake (DE) and Maximum Considered Earthquake (MCE_R) ground motion intensities. These results formed the basis of a comparative assessment of seismic loss metrics and functional recovery timelines, facilitated through the SP3 computational framework. The analysis effectively quantified the improvements in structural resilience and reductions in damage severity attributable to base isolation strategies.

Furthermore, the study highlighted key differences in code-minimum analytical procedures, based on modal response spectrum analysis (MRSA) for fixed-base Special Moment Frames (SMFs), underscoring their limitations in capturing nuanced performance outcomes under extreme seismic loading conditions. The MRSA is without a doubt the most popular methodology for the analysis and design of SMF in the industry up to date. The analytical procedure was developed in 1932 by Biot, and it was first incorporated into the 1994 Uniform Building Code (UBC-94). It is recognized as a more reasonable methodology than the equivalent lateral force procedure (ELF), also more computationally expensive, which was originally intended to better capture the demand for the lateral force resisting system (LFRS), or primary system, for tall buildings and buildings with uneven distribution of mass with a linear elastic- isotropic material structural approach, appropriate for the 1930's, and has been extended with time to other parts of the buildings like diaphragms and non-contributing gravity force resisting system (GFRS). The implementation of MRSA motivated the development of the software and computational power in structural design. Although MRSA has been used extensively for design with the main objective of life safety and collapse prevention, it may not be the best tool for evaluating seismic performance and resilience compared to using NLRHA. The computing power and capabilities of modern computers have increased tremendously in the last 50 years, plus the amount of earthquake accelerograph records that are available have made it more feasible to perform NLRHA.

Building Description

Three hypothetical buildings of identical floor plan above ground are studied, as shown in Figure 1(a). The buildings are located at a site in Century City, Los Angeles, California, USA, in an area with high seismicity and at a site having seismic Site Class C in accordance with ASCE 7-16 or Site Class CD in accordance with ASCE 7-22. The buildings have six stories above ground, a typical story height of 12 ft, and total height above ground of 72 ft. All three structures utilize six bays of moment frame in the X-direction and eight bays of moment frame in the Y-direction. It was assumed that the X-direction of the buildings is parallel to the fault-normal direction (i.e. the direction with higher ground motions).

The fixed-base (FB) Steel - Special Moment Frame (FB-SMF or SMF) and base-isolated SMF (BI-SMF) structures used the same frame sections based on the fixed-based design of a SMF with SidePlate (SP) connections. If design schedule time were more flexible, the BI-SMF building, redesigned to ASCE 7-22 Chapter 17 Seismic Design Requirements for Seismically Isolated Structures, would encompass similar to slightly stiffer cross sections for all SMF beam-column elements in order to strictly comply with the inter-story drift limits for all ground motions. The damped moment frame building (SMF-VD) used different frame sections based on a reduced base shear and ignoring drift demands in the linear design process (discussed more thoroughly in the design section below). Table 1 summarizes the column and beam sections of the X-direction for the different buildings.

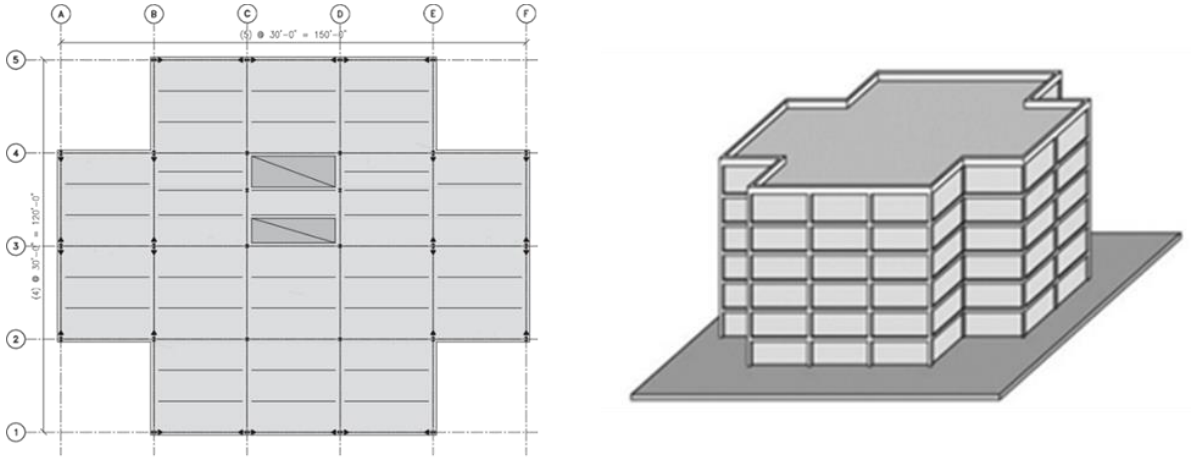

(a) (b)

Figure 1. (a) Floor framing plan; (b) Isometric (3D) view of the buildings above ground.

Table 1. Column and beam sections in the X-direction for the three evaluated structures.

	FB-SMF		BI-SMF		SMF-VD	
	Columns	Beams	Columns	Beams	Columns	Beams
Story 6	W24x103	W21X40SP	W24x103	W21X40SP	W24x76	W18x40 SP
Story 5	W24x103	W21X50SP	W24x103	W21X50SP	W24x76	W18x40 SP
Story 4	W24x103	W21X50SP	W24x103	W21X50SP	W24x76	W18x40 SP
Story 3	W24x103	W24x62SP	W24x103	W24x62SP	W24x76	W18x40 SP
Story 2	W24x131	W24x62SP	W24x131	W24x62SP	W24x76	W18x40 SP
Story 1	W24x131	W24x62SP	W24x131	W24x62SP	W24x94 (ext.) W24x103 (int.)	W18x40 SP

The buildings are classified as Risk Category II in accordance with IBC and ASCE 7 standards. Each structure comprises approximately 15,220 square feet of floor area constructed using composite concrete-filled metal decking, supported by ASTM A992 Grade 50 steel wide flange beams, girders, and columns with welded shear connectors. Floor plates utilize ASTM A572 Grade 50 weldable steel, and the deck incorporates grade 50 light-gauge metal filled with concrete specified at 4,000 psi nominal compressive strength. Non-structural exterior walls along the perimeter have a unit weight of 19 psf, while interior partitions weigh 20 psf. The seismic weight of the superstructure of the buildings is approximately 8,100 kips and, in the case of the BI-SMF building, the isolation slab weighs an additional 1107 kip.

Ground Motions

Ground motions were developed for the hypothetical buildings situated in Century City, a location with high seismic hazard. In accordance with ASCE 7-22 (ASCE 7), the site is classified as Seismic Site Class CD based on prior measurements indicating a shear wave velocity ($V_{S\,30}$) of 420 m/s. For reference, the site would be classified under the previous edition of ASCE 7, ASCE 7-16, as Seismic Site Class C.

ASCE 7-22 mapped seismic parameters are S_S = 2.35, S_1 = 0.85, S_{MS} = 2.47, S_{M1} = 1.55, S_{DS} = 1.65, and S_{D1} = 1.03. ASCE 7-16 mapped seismic parameters are S_S = 2.24, S_1 = 0.82, S_{MS} = 2.24, S_{M1} = 1.07, S_{DS} = 1.49, and S_{D1} = 0.72. Site-specific spectra (developed as described below) yielded S_{MS} = 2.576, S_{M1} = 1.419, S_{DS} = 1.718, and S_{D1} = 0.946.
To perform a site-specific ground motion study, a probabilistic seismic hazard analysis (PSHA) was performed using UCERF 2 and 3, with deterministic spectra developed for seven faults including the Newport-Inglewood, Santa Monica, Hollywood, and Compton Thrust Faults based on proximity and hazard significance (the proximity of the hypothetical location to the Newport-Inglewood, Santa Monica, and Hollywood faults results in a near fault condition which although not explicitly defined in ASCE 7-16 nor ASCE 7-22, nevertheless should be incorporated into the ground motion evaluation, and produces relatively high accelerations). The ground motion study employed ground motion prediction equations (GMPEs) and directivity models [17, 18]. At each period, the deterministic spectrum was taken as the maximum spectral ordinate from each of the deterministic spectra. The results of the probabilistic and deterministic spectra are the same whether using ASCE 7-16 or ASCE 7-22.

MCE_R spectra were derived by comparing probabilistic and deterministic results per ASCE 7 Section 21.3; the design spectrum is computed as two-thirds of the MCE_R spectrum and is also required to exceed 80% of the GPS spectrum at all periods. The final MCE_R spectrum is shown in Figure 2.

Eleven seed ground motion pairs were selected and scaled/modified to match the MCE_R spectrum, using NGA West2 protocols as described below. Candidate records were categorized as (a) pulse-type, (b) non-pulse-type, and (c) distant. Hazard disaggregation supported selection of 8 local and 3 distant records, with at least 6 pulse-type records identified per [16, 19], exhibiting pulse periods T_p between 2–7 seconds. To preserve event variability, no more than one record was selected per earthquake. Table 2 summarizes the chosen records and selection criteria.

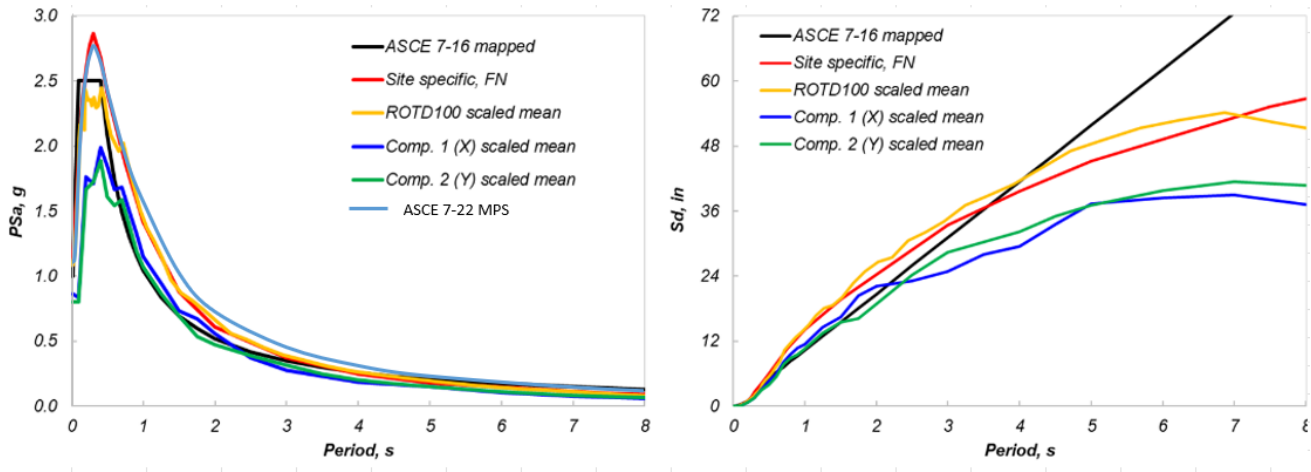

Figure 2. Site-Specific MCE_R.

A hybrid approach was used for scaling/matching of records: for the two non-pulse near-source records and the three distant records selected for this study, pure scaling was performed; the six pulse records were matched using the mean spectral matching approach described in [20]. To ensure spectral compatibility, suites of eight near-source and three distant time histories were evaluated separately, as each corresponds to a distinct target MCE_R spectrum. Figure 3 presents the RotD100 response spectrum for each record pair and the average of the RotD100 spectra. It should be noted that the selected and scaled/matched motions could be used in this case equally well for both ASCE 7-16 or ASCE 7-22 criteria.

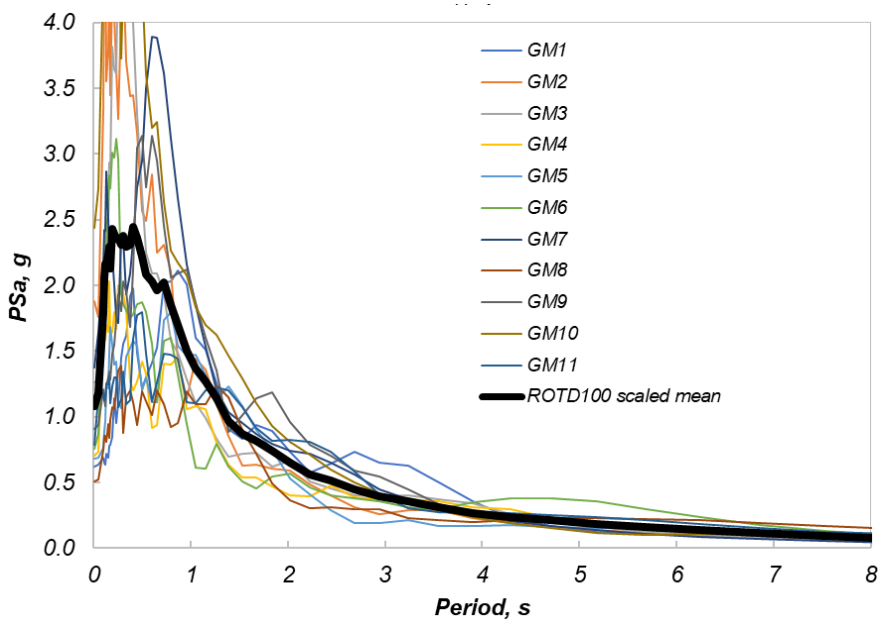

Figure 3. Acceleration spectra of the eleven scaled at MCE_R ground motions.

Table 2. Seed Time-Series for use with MCE_R Response Spectra.

Record No.	NGA RSN No.	Event	Year	Station	M_w	R_{jb} (km)	V_{s30} (m/s)
1	1182	Chi Chi	1999	CHY006	7.62	9.8	438
2	828	Cape Mendocino	1992	Petrolia	7	8.2	422
3	6906	Darfield	2010	GDLC	7	1.2	344
4	900	Landers	1992	Yermo Fire Station	7.28	23.6	354
5	4228	Niigata	2004	NIGH11	6.63	8.9	375
6	143	Tabas	1978	Tabas	7.35	1.8	767
7	5818	Iwate	2008	Kurihara City	6.9	12.9	512
8	4031	Sam Simeon	2003	Templeton 1-story Hospital	6.52	6.2	411
9	1762	Hector Mine	1999	Amboy	7.13	41.8	383
10	5816	Iwate	2008	Shinmachi	6.9	42	359
11	3677	Taiwan SMART1	1986	SMART1 M09	7.3	55.9	322

Seismic Design of the Fixed Base Steel Special Moment Frame (FB-SMF)

The lateral force-resisting system consists of steel Special Moment Frames (SMF) designed to satisfy the minimum strength and displacement requirements of ASCE 7 and the corresponding referenced standards AISC 341 and AISC 358 in ASCE 7. The seismic design employs a response modification factor R of 8 and a deflection amplification factor C_d of 5.5, in line

with ASCE 7 requirements. The SMF design was governed by drift requirements. The structure exhibits fundamental periods of 1.63 sec and 1.55 sec in the X and Y directions, respectively.

The structural design of the SMF was based on a MRSA procedures and evaluated with using NLRHA. Base shear scaling was governed by a long-period limit $C_u T_a$=1.2 sec, resulting in a code-minimum base shear coefficient C_s=0.10. For the drift analysis, a base shear coefficient C_s=0.074 was used.

Seismic Design of the Base-isolated Steel Special Moment Frame (BI-SMF)

The base-isolated building makes use of twenty-eight triple friction pendulum isolators positioned directly beneath the steel columns of the floor plate, as shown in Figure 4. The superstructure of the BI-SMF design is identical to that of the FB design with a seismic weight, W_s = 8100 kips. The isolation system also includes steel beams and an 8 in. slab connecting the top of the bearings to promote a uniform lateral and vertical motion of the isolation system and absorb P-delta moments produced by the isolator displacement and axial load eccentricity. The seismic weight of the isolation slab is equal to W_i =1107 kip.

Preliminary seismic design of the isolation system—assuming rigid superstructure behavior and lower-bound isolator properties under MCE_R loading—yields an effective isolation period T_{eff}=3.56s, an equivalent viscous damping ratio ζ_{eff}=16% (damping factor B_M=1.38), and a normalized base shear ratio V_b/W=0.22, corresponding to an isolation displacement of 27 in. The MCE_R elastic spectral demands at T_{eff} are 0.31 g and 38.9 in. Although ASCE 7 section 17.4.5 indicates that the effective period of the isolated structure, T_M, should be greater than three times the elastic, fixed-base period of the structure above the isolation system, this requirement is established for the Equivalent Lateral Force procedure (ELF). In this case study and discussed in later sections, the period shift of 3.56/1.60=2.22 still enables seismic isolators to absorb a portion of the lateral displacement demands and reduce internal deformations in the protected structure, higher mode effects, and level of seismic damage that would otherwise result in the very flexible FB-SMF building. Figure 4 illustrates the hysteretic response of the isolation devices for both lower- and upper-bound mechanical properties.

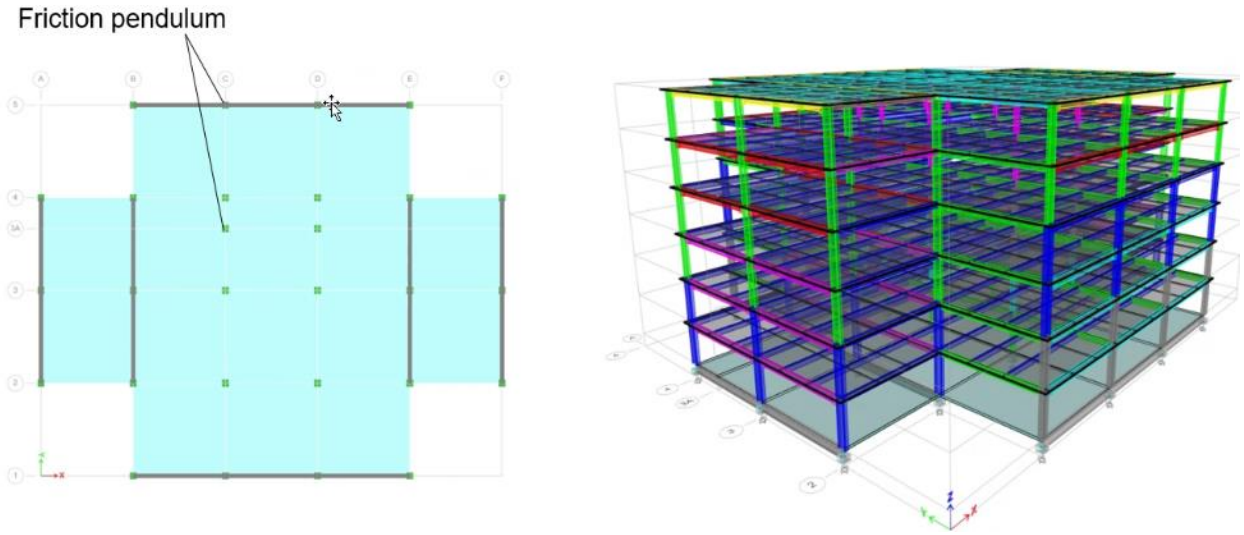

Figure 4. Floor Plan at the Isolation Level with Isolators Layout and 3D View of the Base-Isolated Building - Undeformed Configuration.

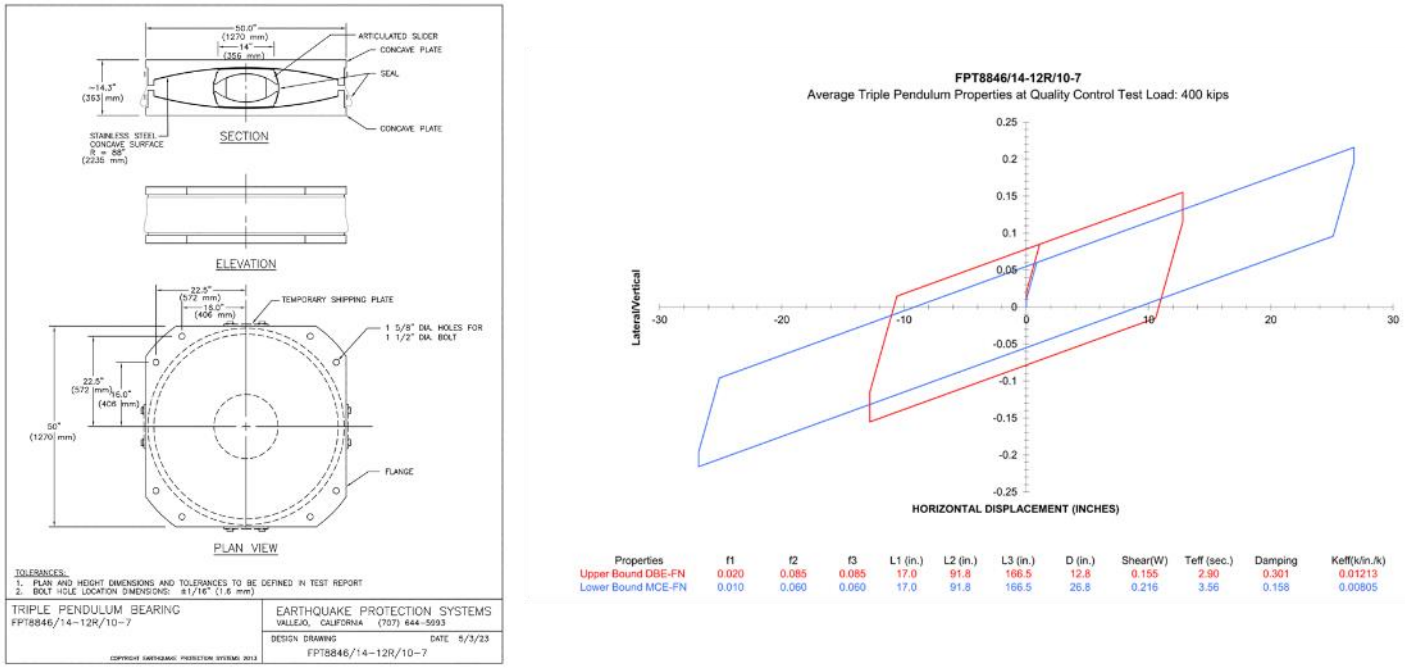

Figure 5. Geometry and Hysteretic Behavior of Friction Pendulums with Lower- and Upper-Bound Property Variations.

The design of the Triple Pendulum bearing included two sets of friction coefficients and radii, equivalent to a double pendulum system. This bearing design was defined with a nominal isolated period limited to approximately 3 seconds to ensure proper recentering of the device with high frictions on main concaves and relatively small plan dimensions, yet primarily to absorb, within the sliding stage of response and without incurring in the isolator stiffening stage, the high seismic demands defined for the study. These design parameters were purposefully selected to reduce construction costs and enable minimum intervention in the baseline SMF building design, though not to target continued functionality of the hypothetical office building selected for the study, classified as Risk Category II structure. Although reduction of construction costs is not explicitly targeted in ASCE 7-22 Chapter 17 for seismically isolated structures, by establishing similar interstory drift ratio (IDR) limits and other structural design criteria to conventional constructions, as well as similar performance goals, typical base isolation design practice can achieve reduced construction cost or slightly enhanced seismic performance (Life Safety in lieu of Collapse Prevention) when applied to a set structural system design.

Seismic Design of the Steel Special Moment Frame with Supplemental Damping (SMF-VD)

For the Steel Special Moment Frame with supplemental damping provided by Fluid Viscous Dampers (FVDs), the moment frame sections were first designed for strength only, using a reduced base shear. Modal Response Spectrum Analysis was used with a base shear scaled to 75% of the Equivalent Lateral Force (ELF) base shear, consistent with the largest reduction in base shear permitted by ASCE 7 Section 18.2.1.1. The design of this frame ignored drift criteria, which would later be addressed by the implementation of FVDs in the NLRHA.

Four FVDs were placed on each floor in both principal directions as shown in Figure 6. In the X-direction, chevron damper configurations were used (Figure 7a) and in the Y-direction, diagonal damper configurations were used (Figure 7b). Dampers were placed outside of the moment frame in the Y-direction, but with shared columns with the X-direction frames. In the X-direction, the dampers were placed asymmetrically both in and outside of the moment frame. These damper locations were chosen to demonstrate the variety of placement options for the dampers in relation to the moment frames.

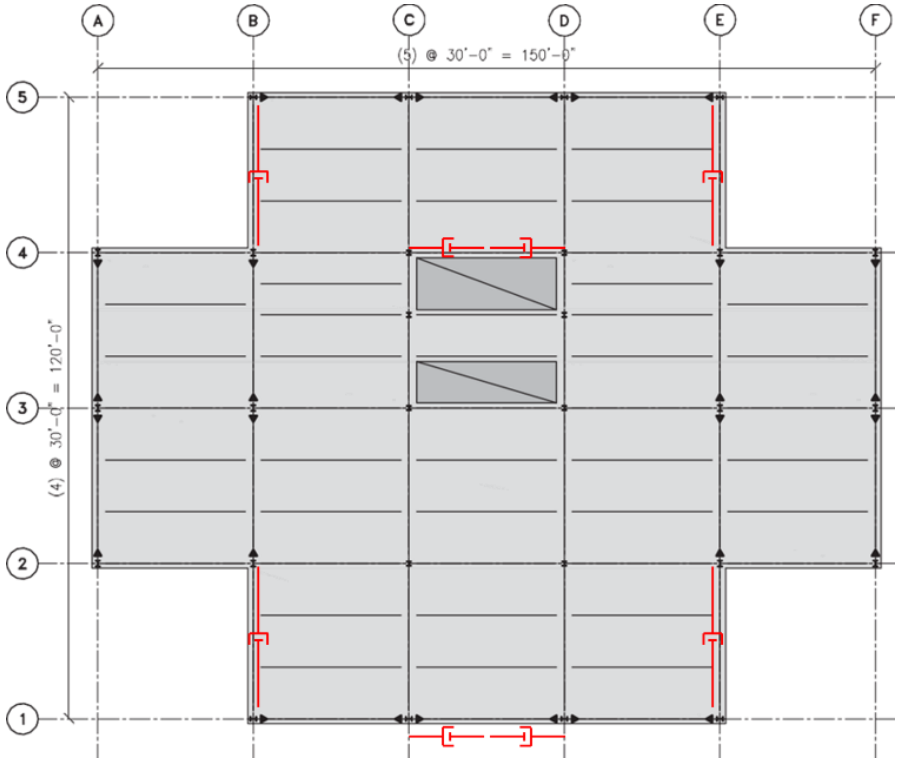

Figure 6. Floor plan showing damper locations in red of the SMF-VD

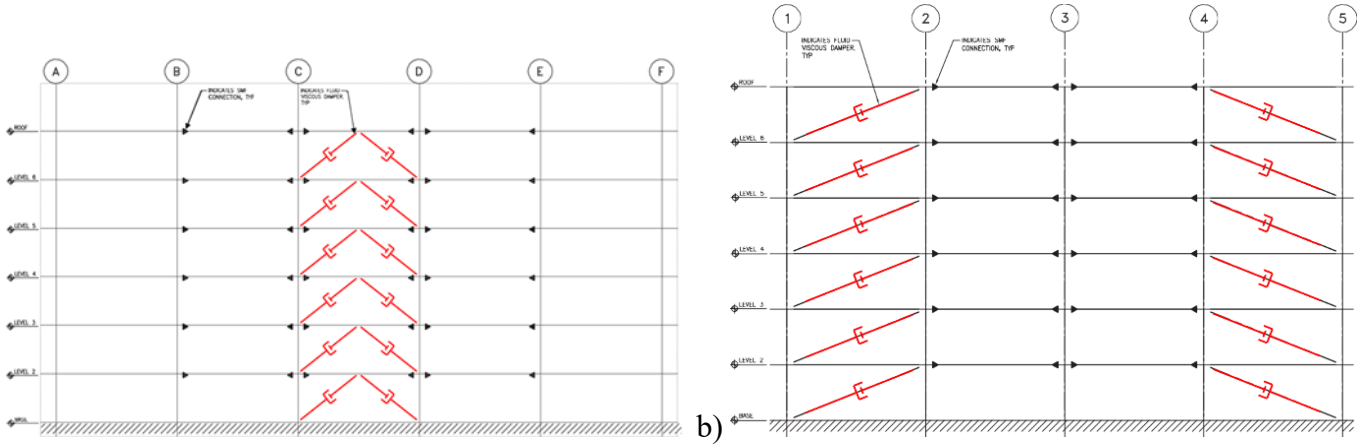

Figure 7. Elevations of damper frames (a) Gridlines 1 and 4 – X-Direction; (b) Gridlines B and E – Y-Direction

FVDs are governed by the following constitutive equation:

$$F = CV^{\alpha} \quad \text{(Eqn. 1)}$$

Where F is the output force, C is the damping constant, V is velocity and α is the velocity exponent. For this design, the velocity exponent was set 0.4 and the damping constants, C, were iterated up the height of the building until the design drift limit of 2% at DE was met in the NLRHA results. The final properties for the dampers, as well as output results of the design force and stroke (corresponding to MCE_R demands) are shown in Table 3. The force demands are based on the

average of the 11 ground motions while the minimum required stroke is based on the maximum stroke from the 11 ground motions – matching industry standards.

Table 3. Final Damper Properties and Design Force and Stroke

	X-Direction					Y-Direction				
Story/ Floor	Quantity	Nominal C	MCE_R Level Force (kips)	Min. Req'd Stroke (± in)	Effective Stiffness for Modeling (k/in)	Quantity	Nominal C	MCE_R Level Force (kips)	Min. Req'd Stroke (± in)	Effective Stiffness for Modeling (k/in)
ROOF	4	46	108	4.5	470	4	35	98	5.2	470
STORY 6	4	61	159	6.1	700	4	35	102	6.1	470
STORY 5	4	61	172	7.1	700	4	53	153	7.3	700
STORY 4	4	107	309	7.1	1400	4	53	151	7.5	700
STORY 3	4	107	293	6.5	1400	4	61	170	7.1	700
STORY 2	4	93	221	3.6	938	4	61	141	3.7	700

Numerical Modeling

Linear and nonlinear response history analyses (NLRHA) were conducted using ETABS Ultimate. The nonlinear structural model incorporated fiber-type P-M2-M3 hinges (as defined in CSI ETABS) at both ends of steel columns and M3 moment hinges at SMF beam ends for all three structures. Structural steel was specified as ASTM A992 Grade 50, with a yield strength of 55 ksi and ultimate strength of 72 ksi. M3 hinge backbone curves, shown in Figure 8, were derived from average experimental data for Special Moment Frame - SidePlate (SP) connections. Friction pendulum isolators were modeled using Triple Pendulum Isolator link elements, TFP, (see Figure 9). Rayleigh damping, compatible with NLRHA, was applied with initial stiffness-based damping coefficients, targeting 0.5% modal damping at 0.05 sec and 8 sec periods.

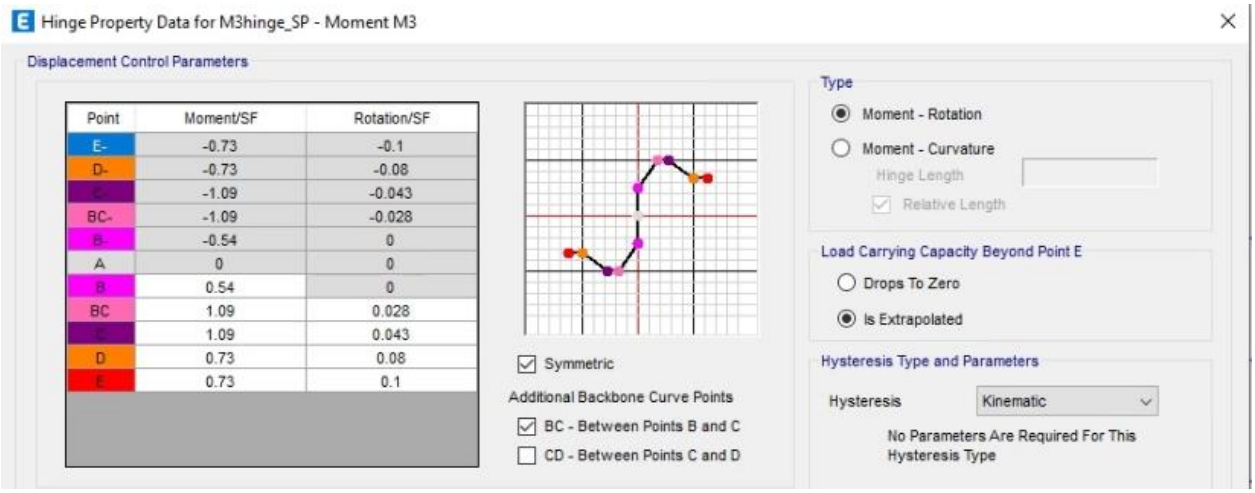

Figure 8. Normalized moment versus plastic rotation of the M3 hinges of SP connections for ETABS.

	Outer Top	Outer Bottom	Inner Top	Inner Bottom	
Stiffness	372	372	96	96	kip/in
Friction Coefficient, Slow	0.057	0.057	0.013	0.013	
Friction Coefficient, Fast	0.085	0.085	0.02	0.02	
Rate Parameter	1.25	1.25	1.25	1.25	sec/in
Radius of Sliding Surface	88	88	12	12	in
Stop Distance	100	100	100	100	in

Figure 9. Parameters definition of the triple friction pendulum isolator link for ETABS.

The FVDs were modeled using Damper – Exponential link elements with nonlinear directional properties in the U1 direction. Lower-bound damping coefficients (C) were used to capture the worst-case analysis related to drift. A lower bound factor, λ_{min}, of 0.85 was used to reduce the damping coefficients. The effective stiffness of the damper (the Maxwell Stiffness) combined with an approximation of the extender brace was used for the stiffness input in the nonlinear properties. These effective stiffness values are shown in Table 3.

Seismic Analysis Results

This section presents the nonlinear response history analysis (NLRHA) results for the Special Moment Frame (SMF), and the Base-Isolated (BI-SMF) and the SMF with supplemental damping (SMF-VD) designs per ASCE 7. Figure 10 compares mean interstory drift ratios (IDR), story shear demand (V_b), normalized to seismic weight (W_s), V_b/W_s, and floor accelerations for both DE and MCE_R levels. The SMF was originally designed using MRSA to reflect the state of the practice of common SMF designs and was analyzed with NLRHA to evaluate the performance and the seismic response of the SMF . The NLRHA results of the SMF indicate that the design meets the strength provisions of ASCE 7, but suggests that the average IDR at DE (2.45%) is slightly higher than the 2% interstory drift limit per the code requirements for the MRSA which does not imply a non-compliant IDR as the ASCE 7 Chapter 16, Section 16.4.1.2 does not include a specific limit in the IDR at DE but at MCE_R For the BI-SMF, the 2% IDR limit set for average nonlinear response history analysis results at the MCE_R level is established in ASCE 7-22 Section 17.6.4.4 (2) for the structure above the isolation system.

Across all parameters and seismic intensities, base isolation yields substantial reductions, ranging from 33% to 66%. Under DE loading, the fixed-base SMF (SMF) design shows a peak IDR of 2.45%, which is 22% higher than the 2% estimate from code-minimum MRSA, attributed to the conservative $C_d/R=0.69$ ratio used in the code. The base shear ratio $V_b/W_s=0.24$ from NLRHA is 2.4 times larger than that from the code-minimum analysis, which could be expected given the differences in the analyses procedures., Floor accelerations exceed 0.64 g at all levels, with a roof acceleration of 1.27 g and PGA of 0.56 g. BI-SMF design achieves over 40% reduction in IDR, greater than 50% reduction in floor accelerations, and more than 34% reduction in story shear, reaching 44% at the base. SMF-VD design exhibits reductions at some levels for IDR, between 5% and 30%, for base shear, between 10% and 40%, and a more significant reduction in floor accelerations, comparable to accelerations obtained for the BI-SMF, between 30% and 45%. While the floor accelerations for SMF may be high enough to prevent a continuous functionality, the floor accelerations observed for BI-SMF and SMF-VD are within tolerable accelerations, approximately below 0.4g, and may be adequate to maintain continuous functionality with a limited disruption.

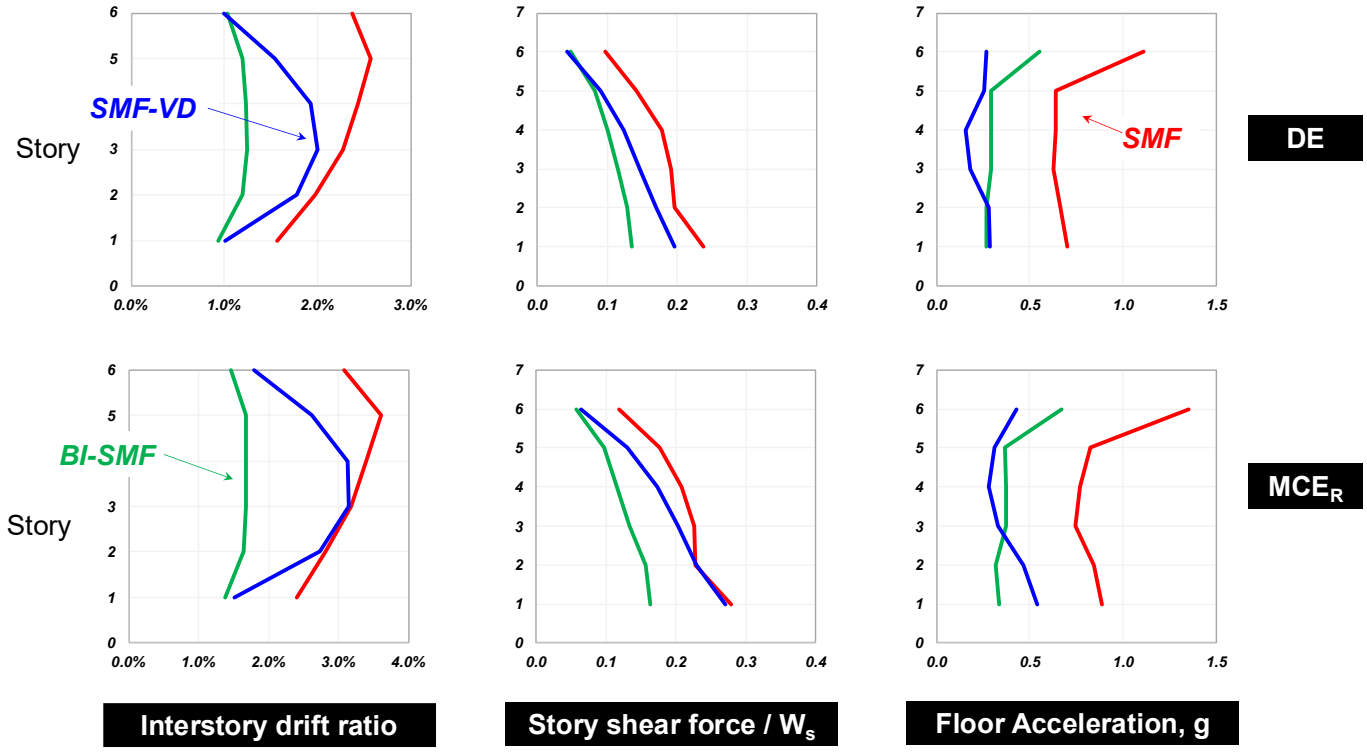

Figure 10. NLRHA response profiles (mean of 11 ground motions) for the SMF, BI-SMF (upper-bound), and SMF-VD (lower bound) buildings at DE and MCE_R.

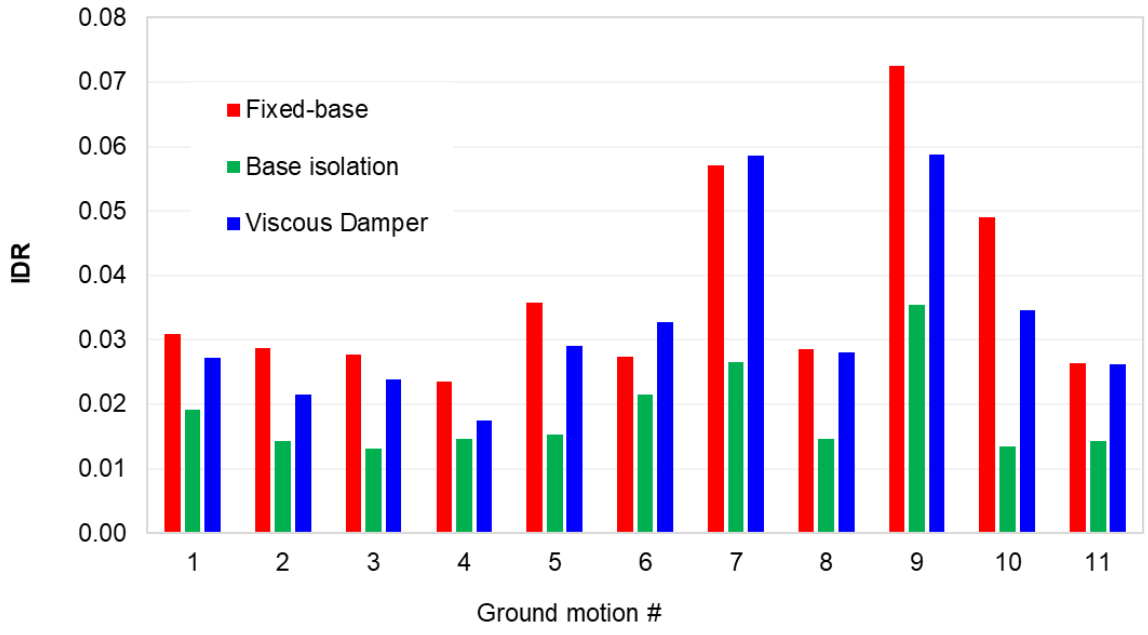

Figure 11. Peak IDR of the SMF, BI-SMF and SMF-VD buildings for each of the eleven ground motions at MCE_R.

Under MCE_R loading, the fixed-base SMF (SMF) design exhibits a peak interstory drift ratio (IDR) of 3.6%, a base shear coefficient V_b/W_s=0.28, and floor accelerations ranging from 0.74 g to 1.36 g. The design with base isolation (BI-SMF) significantly mitigates seismic response—reducing IDR and floor accelerations by over 43% and 50%, respectively, and lowering story shear forces by more than 43% across all levels. The results from the design with supplemental damping (SMF-VD) reflect a marginal reduction of the peak IDRs and shear force demand, with respect to the SMF solution, between 10% and 50% at other levels, at the same time provide a significant reduction of floor accelerations leading to results comparable to BI-SMF. The NLRHA results reinforce the effective performance of BI-SMF and SMF-VD when functionality is sensitive to the project.

Figure 11 illustrates the effectiveness of isolation by plotting peak IDRs for each of the eleven MCE_R ground motions, confirming consistent response reductions. Figure 12 shows the corresponding peak horizontal displacements of the isolation bearings under lower-bound properties, with a mean displacement of 25.2 in. and a maximum of 34.4 in. These NLRHA results align closely with simplified design estimates using the damping modification factor B_M. The stiffening behavior of the Triple Pendulum Element in ETABS was not explicitly modeled, for simplicity, beyond the free sliding capacity of 31 in. (end of stage 4), where the end of the stiffening portion (end of stage 5) of 34 in. and total isolator displacement capacity of 38 in. are disregarded. However, although for two ground motions, displacement demands slightly exceed 31 in., the small increment with respect to this limit indicates that the stiffening behavior of the isolator would have resulted in only slightly higher IDRs, story and base shears, and internal ductility demands in the SMF than those computed, and the overall NLRHA average results and loss estimates were not expected to be significantly affected.

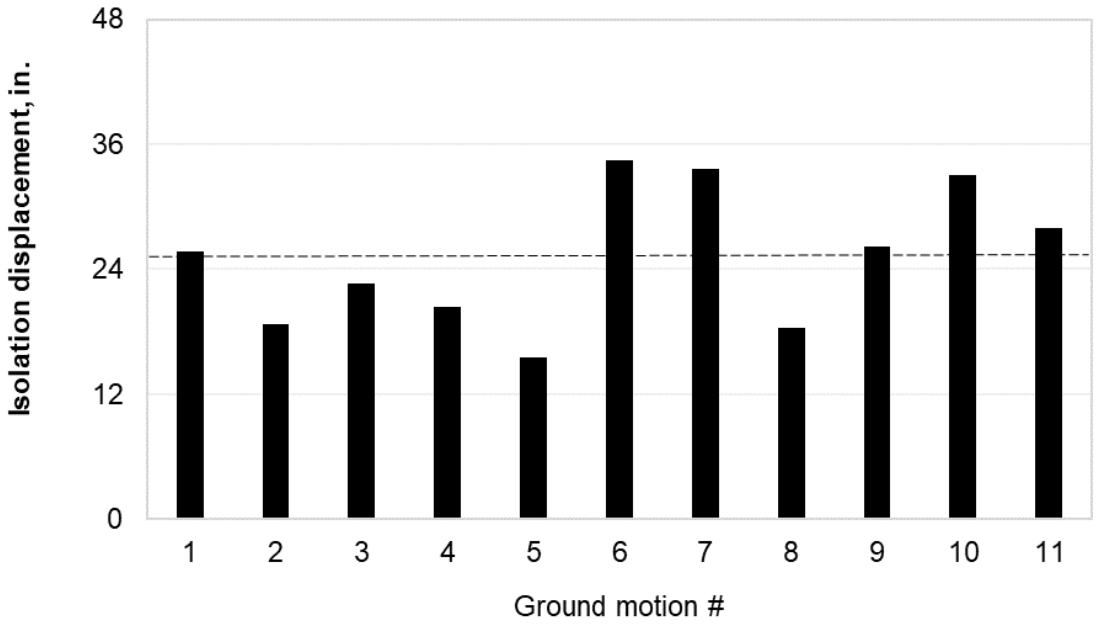

Figure 12. Peak horizontal displacement of the friction pendulums of the BI-SMF (lower-bound) building for each of the eleven ground motions at MCE_R.

Loss and Downtime Analysis

To assess and compare the resilience of the three building designs, economic loss and recovery time are evaluated using the SP3 Risk Model [20], a tool developed by Haselton Baker Risk Group, LLC based on the probabilistic FEMA P-58 [21] methodology for economic loss estimation and the ATC-138 [22] methodology for recovery time analysis.
Input to the SP3 risk model analysis includes general information about the building location, configuration, occupancy, design criteria, structural systems, and non-structural components. Non-structural components for the office building are assumed to include the following items designed to current code requirements:

- Fully glazed exterior cladding
- Light gauge metal stud partition walls with gypsum board sheathing
- Suspended lights and acoustical ceilings
- Steel stairs, Traction elevators, Fire sprinklers
- Potable and non-potable water piping
- HVAC system with a water chiller, cooling tower, and large-diameter ducting
- Back-up battery/generator system and electrical distribution panels

Based on this information, default information in SP3 is relied on to perform the loss and downtime analyses for a suite of earthquake hazards with return periods ranging from 50 to 2475 years.

The structural responses important to the analysis include peak floor accelerations, peak story drifts, and residual drifts. Peak floor accelerations and peak story drifts are computed in the NLRHA structural analysis described previously and input into the risk model for each of the eleven ground motions. Default SP3 approximations are relied upon to compute residual drifts.

The building's fundamental period is close to 2 seconds. Structural analyses were performed for hazards with return periods of 475 and 2475 years. Responses at other return periods are interpolated based on the hazard curve of the 2-second spectral acceleration for all responses except for the ground acceleration for fixed-base models, which is interpolated based on the peak ground acceleration hazard curve.

The downtime analysis includes the following assumptions:

- Inspection, financing, permitting, engineering design, contractor mobilization, and long lead times will all be factors that could delay the start of repairs.
- The building owner does not have an engineer, inspector, or contractor on retainer to help in the event of an earthquake.
- Funding comes from private loans with 2% of building's value available as cash
- HVAC is required for building function, but not for occupancy.
- Plumbing and Electrical are required for building function and occupancy.
- Elevator function is required above three stories.
- Temporary repairs and shoring are allowed to regain occupancy and function.
- The greater of 50% or 2 exits are required for occupancy.
- Flooding consequences are considered.
- Surge demand for material and labor are considered for this building in a dense urban area.

SP3 computes the expected financial loss for a scenario earthquake, expressed as a percentage of the total cost of the building and contents. Figure 13 shows for each building the mean loss, also referred to as the scenario expected loss (SEL); the median loss; and the loss with a 90% non-exceedance probability (NEP), also referred to as the scenario upper

loss (SUL). For the 90% NEP loss, we provide values for both the 90th percentile counted loss and SUL from a curve fitted to values at lower NEP. The counted loss value jumps to 100% once 10% of the realizations in the probabilistic analysis result in a residual drift that exceeds a threshold where the program determines that full building replacement is necessary. Table 4 lists the SEL and fitted SUL values for each building.

The loss values are a combination of contributions from probability of damaged structural components, non-structural components, building collapse, and full-building replacement required by unacceptably large residual drifts. Figure 14 shows the relative contribution of these different sources of loss to the SEL for each of the three buildings.

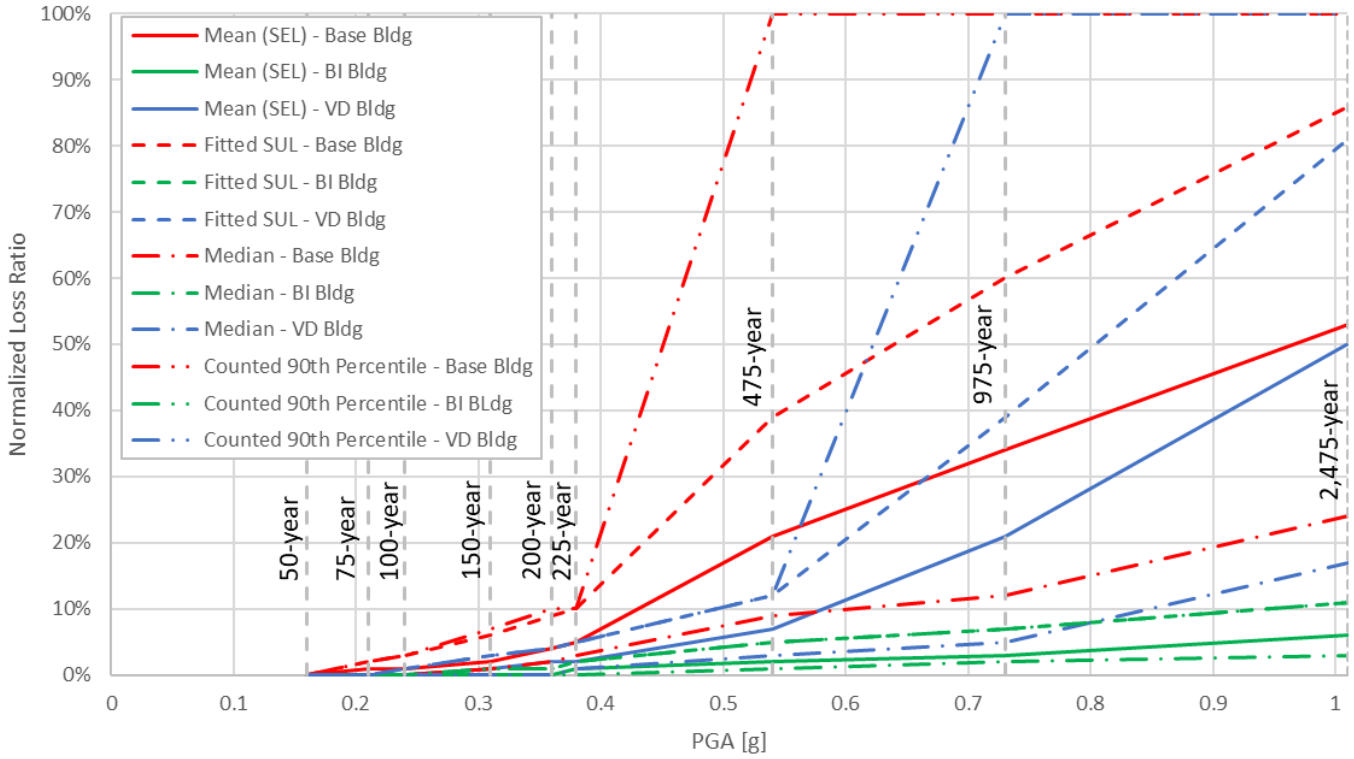

Figure 13. Economic loss comparison for three building types over multiple hazard levels.

Table 4. SEL and SUL for each building type at various hazard levels

Shaking Intensity	Return Period	Base Building		Base-Isolated Building		Viscous-Damped Building	
		SEL (%)	SUL (%)	SEL (%)	SUL (%)	SEL (%)	SUL (%)
63% in 50 years	50 Years	0	0	0	0	0	0
49% in 50 years	75 Years	1	2	0	0	0	0
39% in 50 years	100 Years	1	3	0	0	0	1
28% in 50 years	150 Years	2	6	0	1	1	3
22% in 50 years	200 Years	4	9	0	1	2	4
20% in 50 years	225 Years	5	10	1	2	2	5
10% in 50 years	475 Years	21	39	2	5	7	12

5% in 50 years	975 Years	34	60	3	7	21	39
2% in 50 years	2,475 Years	53	86	6	11	50	81

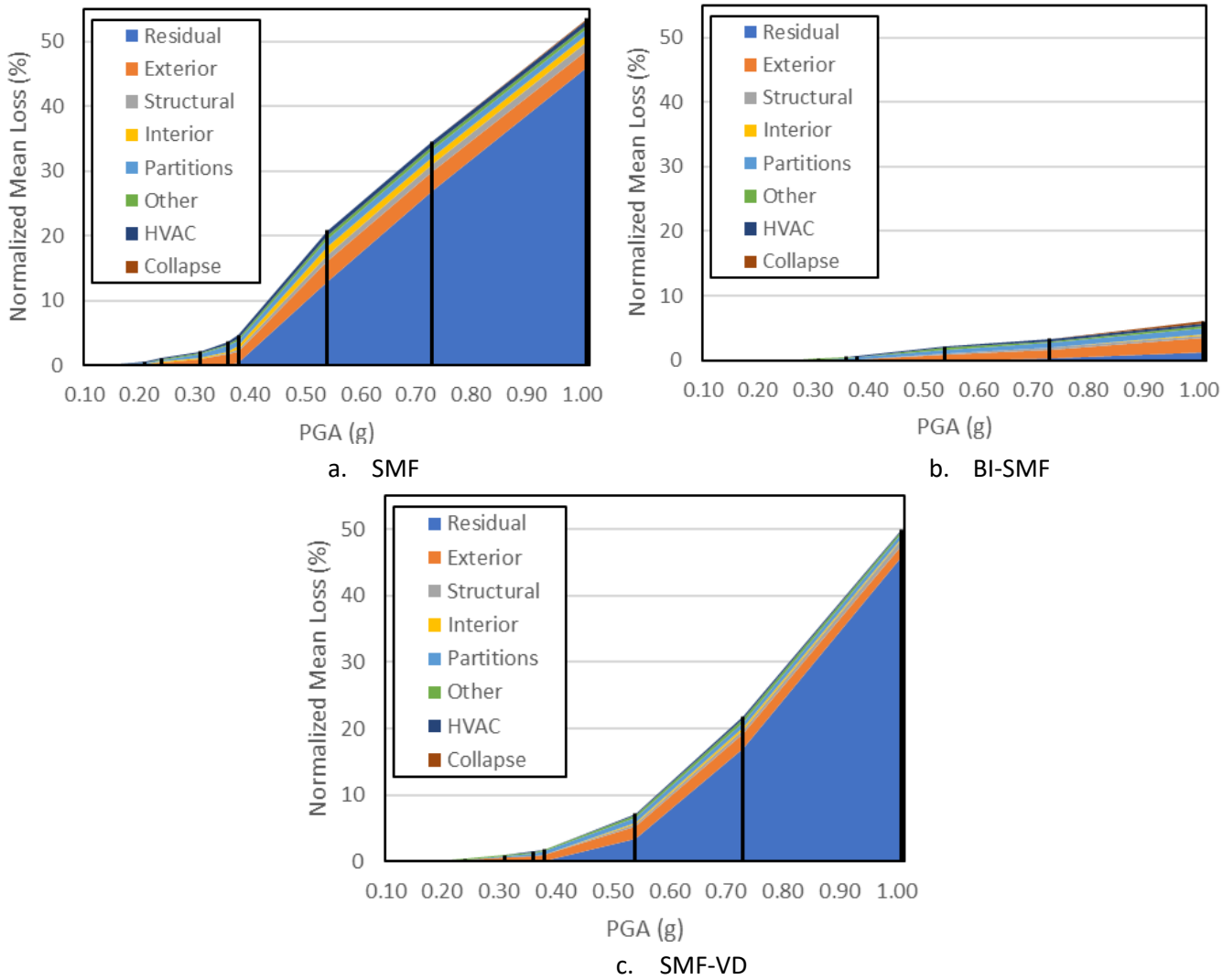

a. SMF

b. BI-SMF

c. SMF-VD

Figure 14. Economic loss comparison for three building types over multiple hazard levels

Figure 15 shows the recovery times for each building over a range of hazards. It is worth noting that even the base-isolated building has a nontrivial recovery time at the 475-year earthquake. To facilitate comparison between the building types, we use the same non-structural components and corresponding fragilities for each building type, using default SP3 fragilities. The partition walls and exterior curtain walls are the most heavily damaged non-structural components, with the median drift corresponding to onset of damage as low as 1%. Recovery times can be significantly improved by specifying non-structural components capable of accommodating larger drifts, providing a design that limits drifts further than what is required by the code, or taking other measures such as having a structural engineer and contractor on retainer to provide expedited post-earthquake repair support.

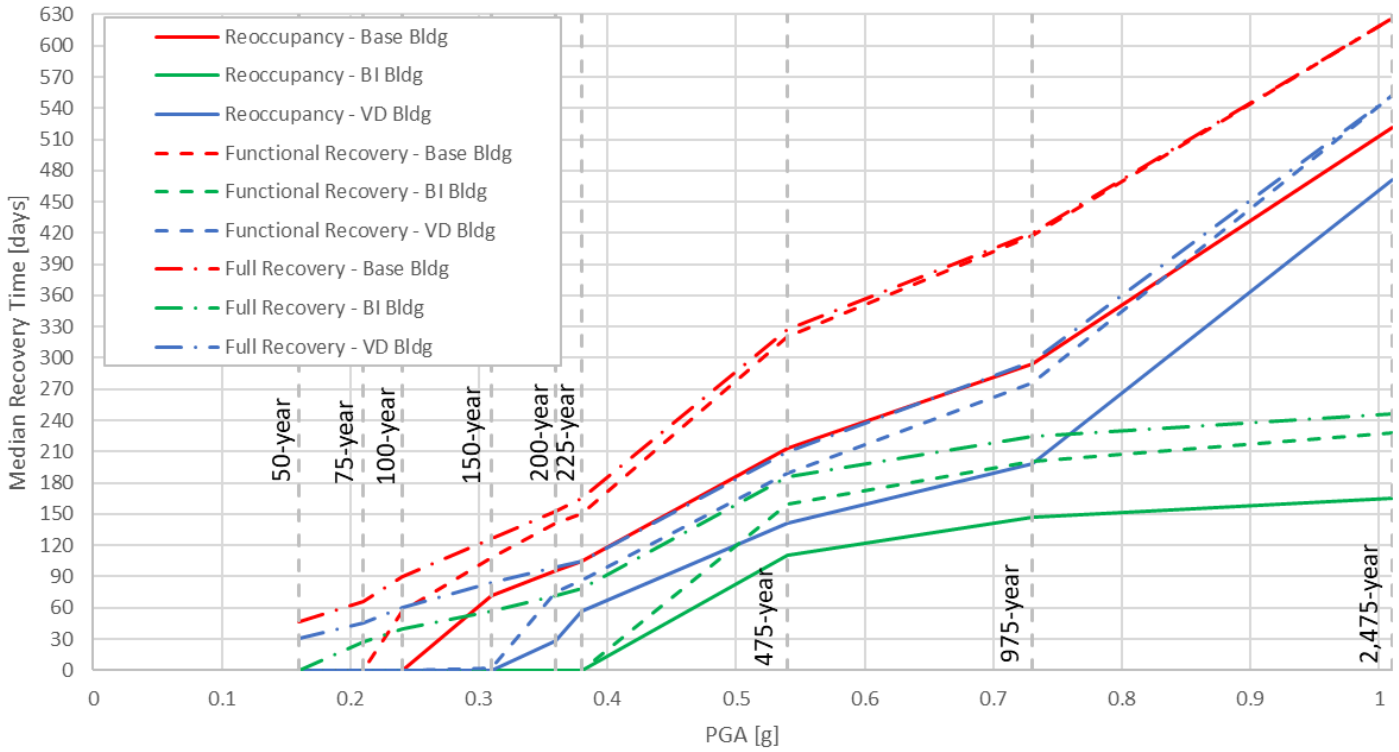

Figure 15. Recovery time comparison for three building types over multiple hazard levels

Conclusions

The fixed-base Steel Special Moment Frame (SMF) and the Base-Isolated Steel Moment Frame (BI-SMF) were designed using linear-modal response spectrum analysis (MRSA) to meet the code-mandated minimum performance requirements. In contrast, the Special Moment Frame equipped with Viscous Dampers (SMF-VD) was sized using nonlinear response history analysis (NLRHA), aligning with the standard industry practice for systems incorporating damping devices. The BI-SMF design leveraged the structural configuration of the SMF and demonstrated a system response modification factor (R) of 1.7. Although this is slightly below the minimum code-specified value of R=2 for base-isolated systems, further design refinement ensured compliance. The MRSA approach was applied to the SMF to reflect common practice in code-based structural design, while NLRHA was used for the SMF-VD building and for refining the isolator performance in the BI-SMF building, particularly for the triple-friction pendulum (TFP) isolators, in line with current state-of-the-practice procedures.

Nonlinear analysis results suggest that the superstructure drifts—and by possible extension, the potential for structural and nonstructural damage—are higher than those predicted by MRSA for select ground motions. This finding highlights a potentially gap between code compliance and expected damageability. Despite satisfying code requirements, the SMF still exhibits considerable susceptibility to damage (structural and nonstructural) under expected seismic loading.

When comparing the SMF and BI-SMF and SMF-VD on an equal-design basis, it becomes evident that even though all meet minimum code provisions, their seismic resilience differs substantially. The results from the design with supplemental damping (SMF-VD) reflect a marginal reduction of the peak IDRs and shear force demand, with respect to the SMF solution, between 10% and 50% at other levels, at the same time provide a significant reduction of floor accelerations leading to results comparable to BI-SMF. The Seismic isolation system, using Triple Pendulum bearings (BI-SMF), were highly effective in reducing seismic demands and achieving enhanced seismic performance in a superstructure consisting of SMF, which design and cross sections were not altered with respect to the fixed-based condition. These enhancements included reductions of approximately 40% in inter-story drift ratio, 50% in floor accelerations, 45% in base shear demands, and 35%

in story shears, as obtained through nonlinear response history analysis at the design level earthquake, Although there appears to be higher than expected drifts in the flexible SMF superstructure on isolators (2.57% IDR compared to the 2.0% code-prescribed limit) computed from NLRHA of the building in ETABS, the overall seismic isolation design approach and 3D NLRHA results were consistent with ASCE 7-22 Chapter 17 requirements and targeted performance for a Risk Category II- Ordinary structure.

The NLRHA results reinforce the effective performance of BI-SMF and SMF-VD when functionality is sensitive to the project. The SMF, while effective at preventing collapse due to its ductile behavior and energy dissipation capacity, is not inherently designed to maintain post-earthquake functionality. As such, a more detailed design process using NLRHA and targeting functional recovery objectives is recommended over the traditional MRSA-based code-minimum design. To achieve specific performance objectives, SMF buildings must be designed with stiffer and stronger lateral systems than that required for simple code compliance. On the other hand, systems like SMF-VD and BI-SMF are more commonly evaluated for their ability to enable functional recovery or even maintain continued functionality following earthquakes, and they generally demonstrate enhanced post-earthquake resilience. Clearly, the design of the energy dissipation or seismic isolation systems has to be adjusted for the targeted functionality objective. In contrast, SMFs designed solely with MRSA tend to show more limited functional performance due to their larger drifts and damage levels. At the same time the steel tonnage of the three systems is different, where the SMF-VD is the lowest of the three building designs, and the BI-SMF the highest with the addition of the steel member base level. This can be seen in the frame member weights summarized in Table 1.

Evaluating a building's ability to remain functional after an earthquake typically involves assessing its performance under frequent seismic events, which generally correspond to return periods ranging from 50 to 150 years for ordinary buildings, and up to 475 years for essential facilities. According to the analysis, both SMF-VD and BI-SMF designs targeting Collapse Prevention or Life Safety, at best, experienced limited disruption of functionality in the order of days to a few short weeks when subjected to frequent earthquake ground motions within the 50–150-year return period range and weeks' to months'-long disruption at higher return periods. In contrast, the conventional SMF, although not suffering catastrophic damage, is expected to require a recovery period lasting several weeks to months before regaining full operational capacity at the 50-150-year return period, or several months to years at higher return periods. Although not explicitly detailed in the current paper, construction cost increases with the implementation of seismic protection devices such as viscous dampers and triple pendulum isolators would clearly be compensated for through a reduction in direct and indirect economic losses that could be produced in building structures of any risk category under strong earthquakes and the corresponding repair or replacement costs required to rehabilitate them.

References

1. Mokha AS, Amin N, Constantinou MC, Zayas V (1996). Seismic isolation retrofit of large historic building. Journal of Structural Engineering 122(3) 298-308

2. Komuro T, Nishikawa Y, Kimura Y, Isshiki Y (2005). Development and realization of base isolation system for high-rise buildings. Journal of Advanced Concrete Technology 3(2):233-239

3. Dao, N.D., Ryan KL, Sato E, Sasaki T (2013), Predicting the displacement of Triple PendulumTM bearings in a full-scale shaking experiment using a three-dimensional element, Earthq. Eng. Struct. Dyn. 2013, 42.
4. Mokha A, Zayas V, Low S (2024). Proven criteria for achieving functionality of structures with seismic isolation. 18th World Conference on Earthquake Engineering, WCEE20205, Milan, Italy.

5. Kani N (2009) Current state of seismic-isolation design. Journal of Disaster Research 4(3):

6. Morgan TA, Mahin, SA (2010) Achieving reliable seismic performance enhancement using multi-stage friction pendulum isolators, Earthquake Engineering and Structural Dynamics 39, 1443–1461

7. Kelly JM, Konstantinidis DM (2011) Mechanics of rubber bearings for seismic and vibration isolation, Wiley

8. Mayes RL, Brown AG, Pietra D (2012) Using seismic isolation and energy dissipation to create earthquake-resilient buildings. NZSEE Conference

9. Becker TC, Mahin SA (2012) Experimental and analytical study of the bi-directional behavior of the triple friction pendulum isolator. Earthquake Engineering and Structural Dynamics 41(3):355–73

10. Ryan K, Sato E, Sasaki T et al (2013) Full Scale 5-Story Building with Triple Pendulum Bearings at E-Defense, Network for Earthquake Engineering Simulation, Dataset, Hyogo Earthquake Engineering Research Center (E-Defense), Miki, Japan, DOI: 10.4231/D3X34MR7R

11. Calugaru V, Panagiotou M (2014) Seismic response of 20-story base-isolated and fixed-base RC Structural wall buildings at a near-fault site. Earthquake Engineering and Structural Dynamics, Vol. 43, Issue 6, pp. 927-948

12. Walters M (2015) Seismic Isolation – The Gold Standard of Seismic Protection. Structure Magazine

13. Giammona A, Gemmill M, Navalpakkam S (2022) A new vision for a modern hospital. Structure Magazine

14. American Society of Civil Engineers (2022) Minimum Design Loads and Associated Criteria for Buildings and other Structures: ASCE/SEI 7-22

15. Ramirez, O.M., Constantinou, M.C., Kircher, C.A., Whittaker, A.S., Johnson, M.W., Gomez, J.D., and Chrysostomou, C.Z., 2000, Development and Evaluation of Simplified Procedures for Analysis and Design of Buildings with Passive Energy Dissipation Systems, MCEER Report 00-0010, Revision, 1, Multidisciplinary Center for Earthquake Engineering Research, University at Buffalo, State University of New York, Buffalo, NY, 470 pp.

16. Field EH, Biasi GP, Bird P et al (2012) Selection of near-fault pulse motions for use in design. 15th World Conference on Earthquake Engineering, Lisbon, Portugal

17. Shahi SK, Baker JW (2014) NGA-West2 Models for Ground Motion Directionality: Earthquake Spectra, v. 30, no. 3, p. 1285-1300

18. Bayless J, Somerville P (2013) Bayless-Somerville Directivity Model, Chapter 3 of Pacific Earthquake Engineering Research Center Report PEER-2013/09, P. Spudich (editor), Berkeley, CA

19. Hayden CP, Bray JD, Abrahamson NA et al (2012) Selection of near-fault pulse motions for use in design. 15th World Conference on Earthquake Engineering, Lisbon, Portugal

20. Mazzoni S, Hachem M, Sinclair M (2012) An Improved Approach for Ground Motion Suite Selection and Modification for Use in Response History Analysis. 15th World Conference on Earthquake Engineering, Lisbon, Portugal

21. SP3 Homepage, https://sp3risk.com/, last accessed 2023/8/25.

22. Applied Technology Council (2018) Seismic Performance Assessment of Buildings Volume 1 – Methodology, FEMA P-58, Redwood City, CA

23. Applied Technology Council (2021) Seismic Performance Assessment of Buildings Volume 8 – Methodology for Assessment of Functional Recovery Time, Preliminary Report, Redwood City, CA

24. Biot, M.A. (1932) - Vibrations of Buildings During Earthquake - Chapter II in Ph.D. Thesis No. 259, entitled Transient Oscillations in Elastic Systems, Aeronautics Department, California Institute of Technology, Pasadena, California